Since January 2020 Elsevier has created a COVID-19 resource centre with free information in English and Mandarin on the novel coronavirus COVID-19. The COVID-19 resource centre is hosted on Elsevier Connect, the company's public news and information website.

Virology **269,** 172–182 (2000)
doi:10.1006/viro.2000.0218, available online at http://www.idealibrary.com on IDEAL®

Downstream Ribosomal Entry for Translation of Coronavirus TGEV Gene 3b

Jennifer Black O'Connor and David A. Brian[1]

Department of Microbiology, University of Tennessee, Knoxville, Tennessee 37996-0845

Received September 24, 1999; returned to author for revision November 15, 1999; accepted January 21, 2000

Gene 3b (ORF 3b) in porcine transmissible gastroenteritis coronavirus (TGEV) encodes a putative nonstructural polypeptide of 27.7 kDa with unknown function that during translation *in vitro* is capable of becoming a glycosylated integral membrane protein of 31 kDa. In the virulent Miller strain of TGEV, ORF 3b is 5′-terminal on mRNA 3–1 and is presumably translated following 5′ cap-dependent ribosomal entry. For three other strains of TGEV, the virulent British FS772/70 and Taiwanese TFI and avirulent Purdue-116, mRNA species 3–1 is not made and ORF 3b is present as a non-overlapping second ORF on mRNA 3. ORF 3b begins at base 432 on mRNA 3 in Purdue strain. *In vitro* expression of ORF 3b from Purdue mRNA 3-like transcripts did not fully conform to a predicted leaky scanning pattern, suggesting ribosomes might also be entering internally. With mRNA 3-like transcripts modified to carry large ORFs upstream of ORF 3a, it was demonstrated that ribosomes can reach ORF 3b by entering at a distant downstream site in a manner resembling ribosomal shunting. Deletion analysis failed to identify a postulated internal ribosomal entry structure (IRES) within ORF 3a. The results indicate that an internal entry mechanism, possibly in conjunction with leaky scanning, is used for the expression of ORF 3b from TGEV mRNA 3. One possible consequence of this feature is that ORF 3b might also be expressed from mRNAs 1 and 2.

Key Words: porcine transmissible gastroenteritis coronavirus; gene 3b; ribosomal scanning; ribosomal shunting.

INTRODUCTION

Expression of coronavirus genes occurs through the synthesis of a 3′ coterminal nested set of mRNAs. Although coronavirus mRNAs are structurally polycistronic (the 3′-most mRNA in many but not all viral species is monocistronic), evidence from studies of translation both *in vitro* and *in vivo* has suggested that most function as monocistronic messages. That is, despite their polycistronic configuration, usually only the 5′-terminal ORF on each is abundantly translated (reviewed in Lai and Cavanagh, 1997, and Luytjes, 1995). The location of some coronavirus genes, however, is not 5′-terminal on any mRNA, which would require that the gene, if expressed, be translated by a mechanism allowing translation reinitiation, leaky scanning, frameshifting, or a downstream entry of ribosomes. Examples of such genes include (1) ORF 1b on mRNA 1, from which a polyprotein is synthesized following −1 ribosomal frameshifting (Brierly *et al.,* 1987; Eleouet *et al.,* 1995); (2) ORFs 3b and 3c on avian infectious bronchitis virus mRNA 3 (Boursnell *et al.,* 1985), from which 7.4- and 12.4-kDa proteins are synthesized following leaky scanning and internal ribosomal entry, respectively (Liu *et al.,* 1991; Liu and Inglis, 1992; Le *et al.,* 1995); (3) ORF 5b on mouse hepatitis virus mRNA 5 (Skinner *et al.,* 1985), from which a 9.6-kDa protein(the E protein) is synthesized (Budzilowicz and Weiss, 1987; Leibowitz *et al.,* 1988), by an apparent internal ribosomal entry mechanism (Thiel and Siddell, 1994); and (4) the I ORF in mRNA 7 of the bovine and mouse hepatitis coronaviruses, from which the I protein is made in the +1 reading frame relative to N (Senanayake *et al.,* 1992; Fischer *et al.,* 1997) following ribosomal scanning (Senanayake and Brian, 1997).

In this study, we examine the mechanism by which gene 3b is expressed from mRNA 3 in the Purdue strain of TGEV and demonstrate that, surprisingly, it may be approached by ribosomes entering internally and not necessarily through a leaky scanning step as would be predicted from mRNA 3 sequence. Gene 3b in TGEV is unusual in that for one strain of virus, the virulent Miller strain (Wesley *et al.,* 1989), it is expressed as the 5′-terminal ORF on mRNA 3–1, whereas in three other strains, the virulent British FS772/70 and Taiwanese TFI strains and the avirulent Purdue-116 strain, it is expressed as the second ORF on mRNA 3 (Britton *et al.,* 1989; Chen *et al.,* 1995; this study) (note mRNA structures in Fig. 1A). The differences in transcription patterns appear to be a function of the canonical TGEV UCUAAAC intergenic sequence positioned 18 nt upstream of gene 3b in the genome, which in the Miller virus totally conforms to the canonical sequence but in the British FS772/70 and Purdue-116 strains is UCUAAA*U* and in the Taiwanese TFI strain is *ACA*AAAC. The nonconforming intergenic sequences apparently fail to promote synthe-

[1] To whom correspondence and reprint requests should be addressed at University of Tennessee, Department of Microbiology, M409 Walters Life Science Building, Knoxville, TN 37996-0845. Fax: (423) 974-4007. E-mail: dbrian@utk.edu.

0042-6822/00 $35.00

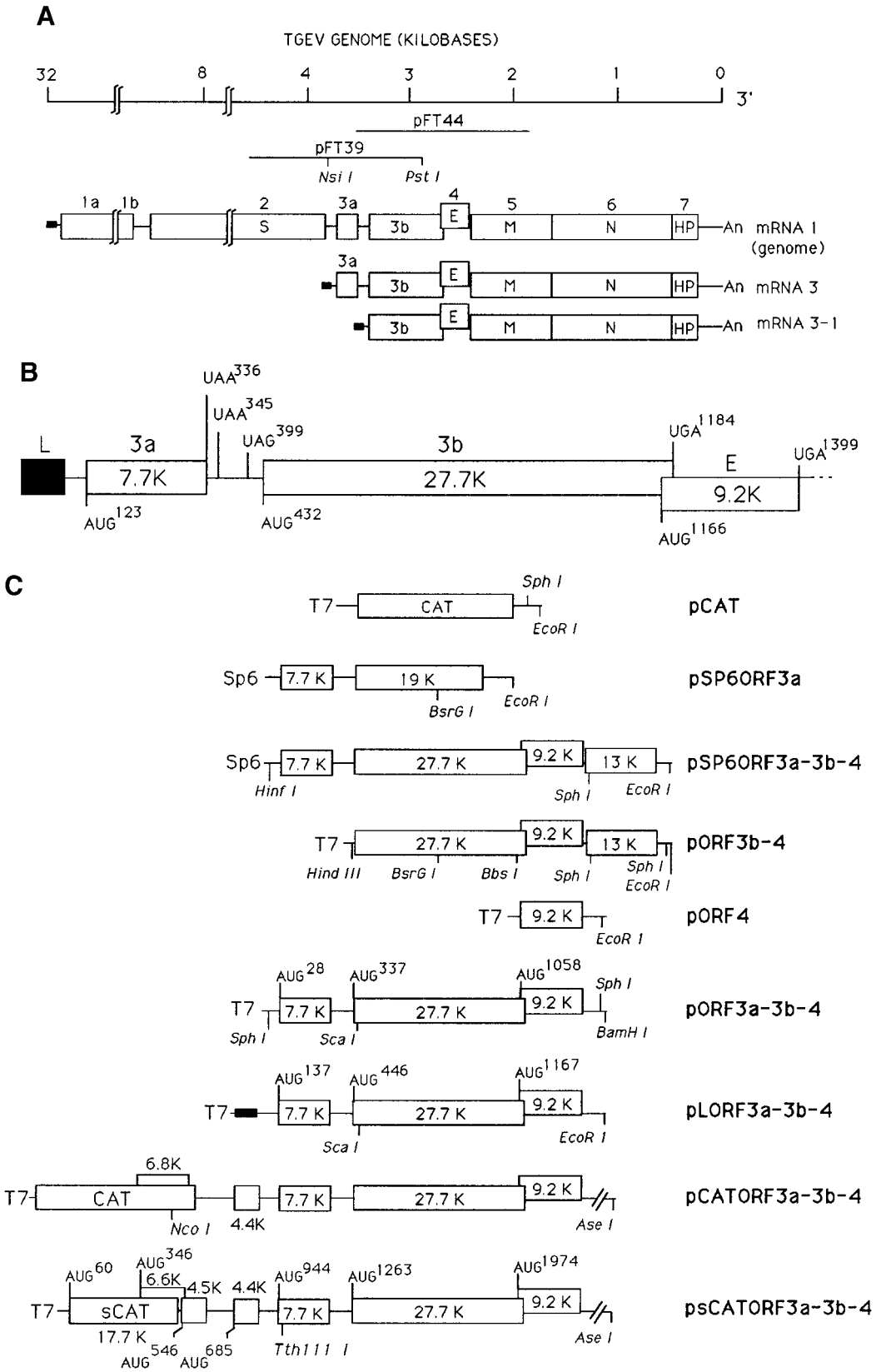

FIG. 1. TGEV genome map and the cDNA constructs used for the expression of gene 3b as a downstream ORF. (A) TGEV genome map showing the positions of cDNA clones FT44 and FT39 from which the expression clones were derived, and the gene maps of mRNA species 1, 3, and 3–1. (B) Map positions of the start and stop codons for ORFs 3a, 3b, and 4 in mRNA 3. (C) cDNA constructs used for the synthesis of RNA transcripts from which translation of ORF 3b was studied.

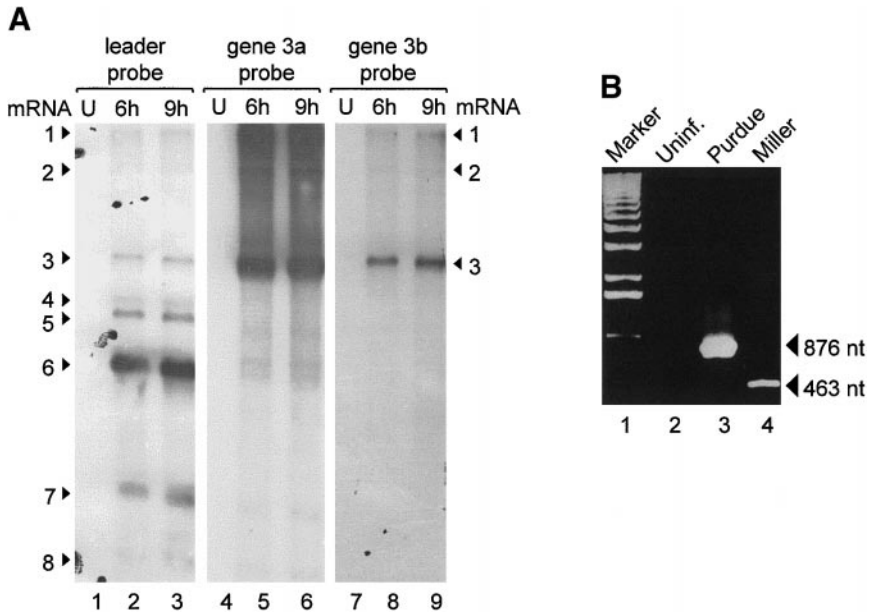

FIG. 2. Northern blot and PCR analyses showing the presence of mRNA 3 but not mRNA 3–1 in cells infected with the Purdue strain of TGEV. (A) Northern blot analysis using gene-specific probes. (B) RT-PCR analysis of RNA from Purdue or Miller virus-infected cells using a plus-strand-detecting oligonucleotide from within ORF 3b as the first primer (for RT and subsequent amplification) and a minus-strand-detecting oligonucleotide from within the leader sequence for amplification. Products were electrophoresed on a gel of 1% agarose and stained with EtBr.

sis of a subgenomic mRNA. Translation from ORF 3b when it occurs as the second ORF on mRNA 3 must, therefore, require either a reinitiation of translation after translation of the upstream ORF, a leaky scanning by ribosomes over a long distance (431 nt; Fig. 1B), or a downstream entry of ribosomes.

Because gene 3b is not intact in some strains of TGEV (i.e., it is either severely truncated by frameshift mutations as in the Purdue-115 strain [Rasschaert *et al.,* 1987] or by deletions as in the avirulent Miller strain [Wesley *et al.,* 1990, 1991]) and cannot produce a full-length product, it has been suggested that its product fulfills a specialized function, perhaps during animal infection (reviewed in Enjuanes *et al.,* 1995), and is not required for virus replication. Similar conclusions were reached after revelations of a truncated gene 3b in strains of the closely related porcine epidemic diarrhea virus (Vaughn *et al.,* 1995). It might therefore be assumed that gene 3b is not translated when it occurs as a downstream ORF as in mRNA 3. However, a product from gene 3b is made in cells infected with the Purdue-116 strain of virus (O'Connor and Brian, 1999), indicating a mechanism must exist for its synthesis from mRNA 3. Here we report that, whereas mRNA 3 has a sequence predicting leaky scanning for the translation of ORF 3b by the model of Kozak (1989), experimental results with mutant constructs suggested downstream entry of ribosomes might also be used. Furthermore, deletion analysis indicated that the internal entry of ribosomes did not depend on an immediate upstream internal ribosomal entry structure (IRES) and suggested ribosomes are entering very close to the ORF 3b start site by a mechanism resembling shunting.

RESULTS

mRNA 3, but not mRNA 3–1, is made in cells infected with the Purdue-116 strain of TGEV

Northern analyses of Purdue-116 virus-infected cells carried out previously in our laboratory with oligonucleotide probes specific for the 3′ end of the genome (i.e., a sequence from within the 3′-proximal HP ORF) had identified eight species of mRNA, leading us to conclude that ORFs encoding the 7.7-kDa (gene 3a) and 27.7-kDa (gene 3b) proteins are each 5′-terminal on separate mRNA species (Sethna *et al.,* 1989). To test this conclusion, separate Northern analyses were done with probes specific for the 90-nt leader and for genes 3a and 3b. Our rationale was that mRNA species 3 and 3–1 would be distinguishable with probes binding within ORFs 3a and 3b because transcripts of 3875 and 3561 nt (or even 4075 and 3761 nt if they included poly A tails of 200 nt in length) are resolvable on a gel of 1% agarose. Northern analyses with the separate probes revealed bands with identical mobilities, indicating the presence of mRNA 3, but not mRNA 3–1, in RNA from Purdue-116 virus-infected cells (Fig. 2A, lanes 4–9).

To test this conclusion by a second method, RT-PCR analysis was done with oligonucleotide primers specific to gene 3b and the minus strand of the leader. Amplified products of 463 and 876 nt would be expected from mRNAs 3–1 and 3, respectively. A product of 5248 nt

might also be found from mRNA 2, the mRNA encoding the spike protein. From RT-PCR analysis only a single product of 876 nt with the proper sequence as determined by cloning and sequencing was obtained (Fig. 2B, lane 3; sequencing data not shown), indicating the presence of mRNA 3 but not mRNA 3–1. To establish that the experimental protocol would have detected mRNA 3–1 if present, RNA was extracted from Miller virus-infected cells and used in parallel. From this, the expected 463-nt mRNA 3–1-derived product was obtained (Fig. 2B, lane 4). No product was obtained with RNA from uninfected cells (Fig. 2B, lane 2).

Genes 3a and 3b, but not gene 4, are translated *in vitro* from synthetic mRNA 3-like transcripts containing all three ORFs

To test by *in vitro* translation whether the 27.7- and 20-kDa gene 3b products (O'Connor and Brian, 1999) are synthesized when ORF 3b is positioned downstream of ORF 3a (beginning at base 337) on synthetic transcripts, uncapped transcripts of pORF3a-3b-4 DNA linearized at the *Bam*HI site 50 nt downstream from the stop codon of gene 4 (Fig. 1C) were translated in either wheat germ extract or rabbit reticulocyte lysate. In both, products from genes 3a (the 7.7-kDa protein containing one methionine) and 3b (the 27.7-kDa form of the protein containing eight methionines and the 20-kDa form presumably containing seven methionines), but not gene 4 (the 9.2-kDa E protein containing four methionines), were obtained (results for wheat germ extract are shown in Fig. 3A, lane 5; note the marker positions in lanes 2–4 and the absence of endogenous product in lane 1). Because a nearly 27-kDa protein was also synthesized from an endogenous transcript in (some) rabbit reticulocyte lysates and the presence of abundant globin protein in the lysate interfered with the resolution of small proteins (data not shown), all subsequent studies described were carried out in wheat germ extract. Thus, from uncapped transcripts bearing similarity to mRNA 3 the first methionine codon in gene 3b (for synthesis of the 27.7-kDa protein) and also the second (assuming synthesis of the 20-kDa protein initiates at the second methionine codon [O'Connor and Brian, 1999]) are accessed for translation. On a molar basis, the amount of 27.7-kDa gene 3b product is approximately one-fifth of that from gene 3a (Fig. 3B). There was no evidence of a 9.2-kDa E protein from ORF 4 in this (Fig. 3A, lane 5) or in subsequent experiments, indicating ribosomal accessibility of ORF 3b was probably not the result of template fragmentation.

An upstream leader-containing sequence in transcripts of pLORF3a-3b-4 (Fig. 1C), although containing an additional 14 nts not found on mRNA 3, had only a small effect on the rate of translation from ORF 3b relative to 3a (Fig. 3A, lane 7, and Fig. 3C), indicating the leader sequence may not strongly influence translation from the downstream ORF; however, this needs confirmation with transcripts precisely mimicking the 5′ end of mRNA 3. As with transcripts of pORF3a-3b-4, no product was evident from ORF 4.

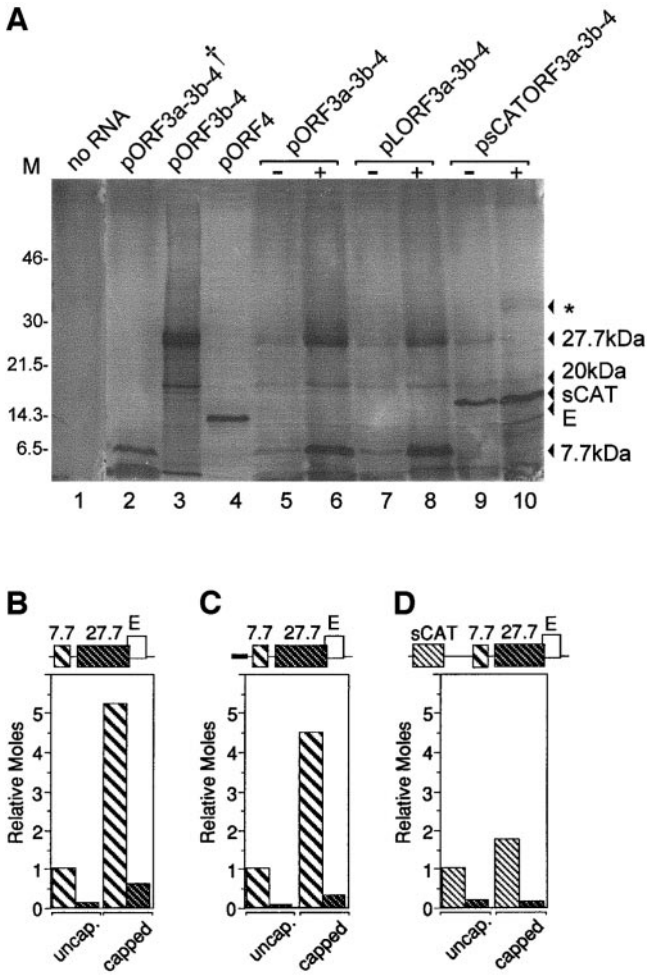

FIG. 3. Effect of a 5′ cap on translation of gene 3b from a downstream position in synthetic transcripts. (A) SDS polyacrylamide gel electrophoresis of radiolabeled translation products. (B, C, and D) Quantitation of products from the indicated constructs as determined from AMBIS radioanalytic imager scans of the gel shown in (A). Note that only detected proteins are represented in the bar graph. * denotes a putative aggregate of the ORF 3b product; † indicates plasmid DNA was linearized at the *Sca*I site within ORF 3b before transcription.

Translation of gene 3b from mRNA 3-like transcripts shows a pattern not fully consistent with a leaky scanning model

From precedents in eukaryotic mRNAs, it is unlikely that ribosomes would approach ORF 3b on mRNA 3 by a mechanism of translation reinitiation, since three in-frame strong stop codons follow ORF 3a (Fig. 1B). However, an approach by leaky scanning according to the model of Kozak (1989, 1991a,b) might be expected, since the initiator codon for ORF 3a (UGU*A123UG*G, in the

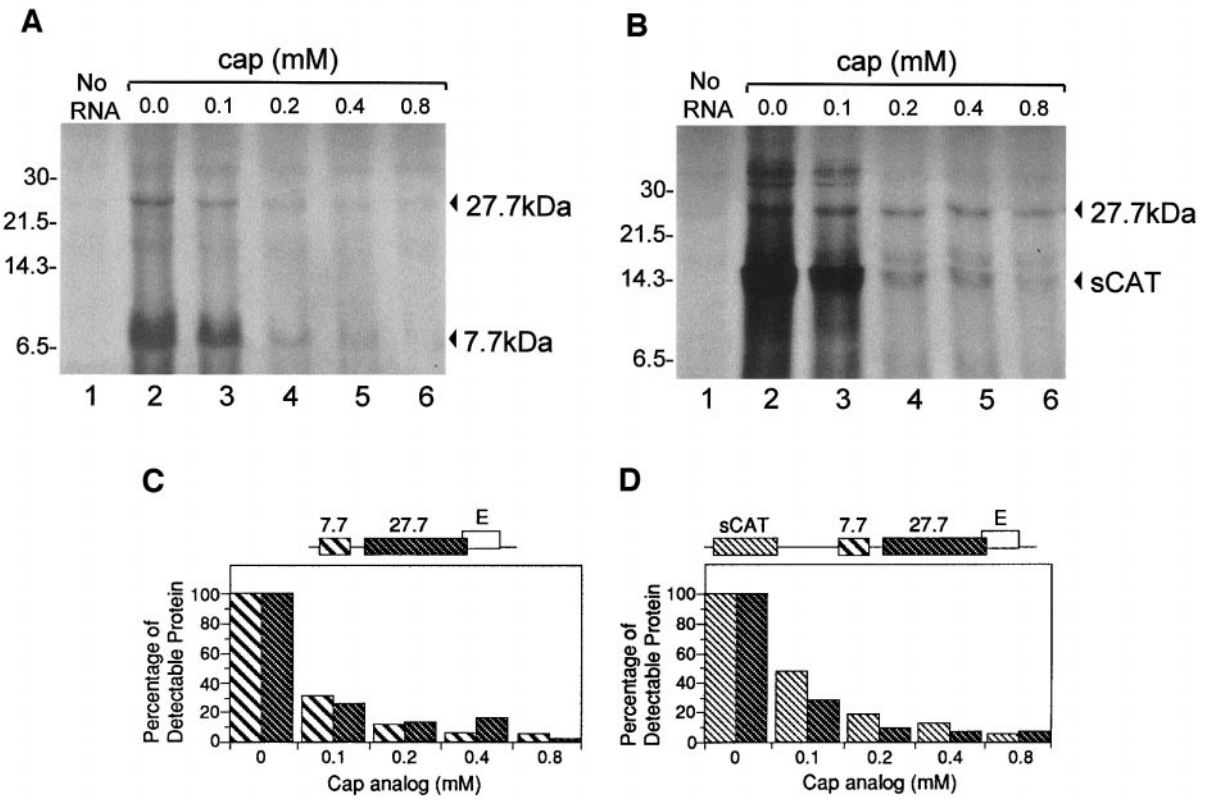

FIG. 4. Competitive effects of soluble methylated cap analog on translation. (A) Results from pORF3a-3b-4. (B) Results from psCATORF3a-3b-4. Radiolabeled products from *in vitro* translation of synthetic transcripts were separated by SDS polyacrylamide gel electrophoresis and bands were quantitated by AMBIS radioanalytic imaging analysis of the dried gel. The quantitated results are shown for pORF3a-3b-4 (C) and for psCATORF3a-3b-4 (D). Note that only detected proteins are represented in the bar graph.

same reading frame as ORF 3b) and for three other potential small ORFs within gene 3a (UAG*A167UG*C, CAU*A283UG*C, and UCC*A424UG*C, all in the +1 reading frame relative to ORF 3b) are within contexts considered weak for initiation, whereas that for ORF 3b (AAA*A432UG*A) is considered relatively strong. To test for ribosomal scanning on mRNA 3-like transcripts, three approaches were taken. In the first, the effect of a 5′ cap on the synthesis of 3a and 3b gene products was measured. Increased synthesis from both would be expected if 5′ cap-dependent entry followed by leaky scanning were used (Kozak, 1989, 1991a). Increased synthesis from 3b might also be expected if a cap-dependent shunting mechanism were used (Jackson, 1996; Mathews, 1996). As can be observed in Fig. 3A, lanes 6 and 8, and Figs. 3B and 3C, enhanced translation of both ORFs 3a and 3b resulted when capped transcripts of pORF3a-3b-4 and pLORF3a-3b-4 were translated. These results are therefore consistent with the mechanisms of leaky scanning and cap-enhanced ribosomal shunting.

In the second approach, the competitive effect of a soluble cap analog on the translation of ORFs 3a and 3b from capped transcripts of pORF3a-3b-4 was measured. With either leaky scanning or cap-dependent shunting, but not with cap-independent internal entry, competitive inhibition of translation from both ORFs would be expected (Iizuka *et al.,* 1994; Jackson, 1996; Mathews, 1996). Nearly the same rate of inhibition was found, 70–75% with 0.1 mM and 85–90% with 2 mM cap analog (Figs. 4A and 4C), indicating either mechanism of cap-dependent entry could be functioning in the translation for ORF 3b.

In the third approach, the sequence context surrounding the 3a start codon in transcripts of pORF3a-3b-4 was modified to become strongly favorable for translation (GCCGCC*ATG*G) (Kozak, 1991b) and the relative amounts of 3a and 3b gene products were measured. With leaky scanning, a diminished synthesis from 3b relative to 3a would be expected regardless of the capped status of the transcripts (Kozak, 1991b), whereas with shunting a change in the relative amounts would not necessarily be expected. As can be noted in Figs. 5A and 5B, whereas the accumulation of 3a product increased almost 20% relative to 3b with the improved Kozak consensus for capped transcripts, no increase was observed with uncapped transcripts. Intriguingly, the absolute amount of gene 3b product appeared nearly identical under all conditions of translation. These results, therefore, are not fully consistent with the leaky scanning model for ORF 3b

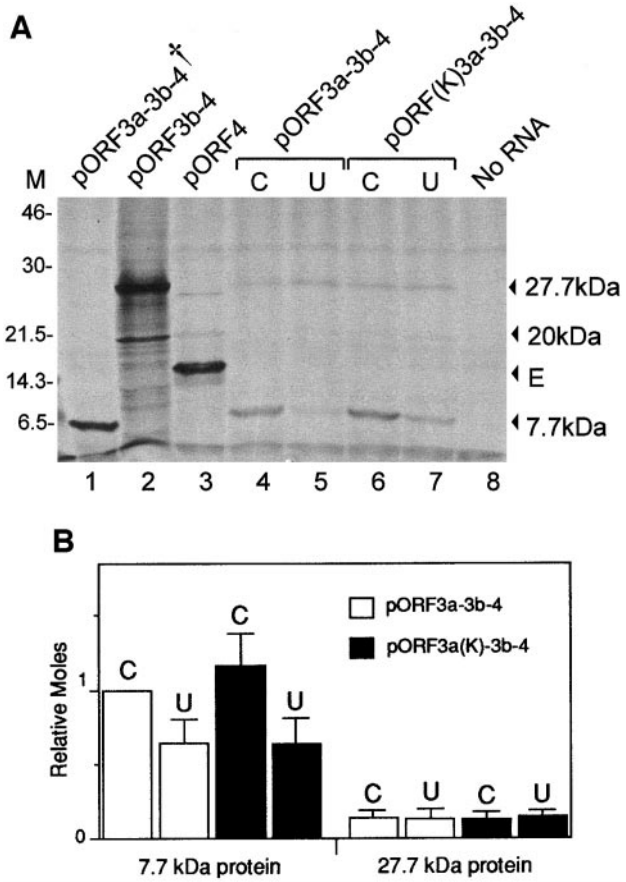

FIG. 5. Effect of an optimal Kozak context for ORF 3a on the translation of ORF 3b. (A) Autoradiogram showing the translation results of capped (C) and uncapped (U) synthetic transcripts of pORF3a-3b-4 (wt, UCCUGU*AUG*G) and pORF3a(K)-3b-4 (optimal Kozak context, GCCGC-C*AUG*G). † indicates plasmid DNA was linearized at the *Sca*I site within ORF 3b before transcription. (B) Quantitation of products as measured by AMBIS scanning. Note that only detected proteins are represented in the bar graph.

translation and suggest the possibility of an internal entry of ribosomes.

Translation of ORF 3b is not blocked by the upstream insertion of an 884-nt-long sequence containing three sequential ORFs

To test for an internal entry of ribosomes onto ORF 3b, pORF3a-3b-4 was modified to psCATORF3a-3b-4 by the placement of an 884-nt-long sequence containing three sequential ORFs upstream of ORF 3a (Fig. 1C) and the products of translation were quantitated. An internal entry of ribosomes, either directed by an IRES element or by a shunting mechanism, would typically not be blocked by the presence of upstream ORFs of this dimension (reviewed in Jackson *et al.,* 1995; Jackson, 1996; Mathews, 1996). Transcripts of psCATORF3a-3b-4 possessed a 5′ UTR of 59 nt; a five-methionine-containing 450-nt sCAT ORF beginning within an excellent Kozak context (AAA*ATG*G) at base 60; a five-methionine-containing 4.4-kDa protein-encoding ORF beginning within a fair Kozak context (ATC*ATG*C) at base 534; a one-methionine-containing 4.5-kDa protein-encoding ORF beginning within a fair Kozak context (CGG*ATG*A) at base 685; and ORF 3a beginning at base 944, ORF 3b beginning at base 1253, and ORF 4 beginning at base 1974. In addition, there is a 66-kDa protein-encoding ORF beginning within a fair Kozak context (TCC*ATG*A) at base 346 within the sCAT ORF (in the +1 reading frame relative to sCAT). All in all, 29 AUG codons exist upstream of ORF 3b. When transcripts of psCATORF3a-3b-4 were translated the following features were noted:

1. From uncapped transcripts, only products from the sCAT and 3b ORFs, in a molar ratio of approximately 1:0.15, were obtained (Fig. 3A, lane 9; Fig. 3D), indicating that among the downstream ORFs, translation from ORF 3b had been a selective one and was probably not the result of initiation on fragmented transcripts.
2. From capped transcripts, an enhanced accumulation from the sCAT ORF was observed but not from the 3b ORF (Fig. 3A, lane 10; Fig. 3D), unless an inexplicable putative aggregated form of ORF 3b (identified by an asterisk in Fig. 3A, lane 10, and noted earlier [O'Connor and Brian, 1999]) was included in the total. (The aggregate was not included in the bar in Fig. 3D.)
3. From capped transcripts in the presence of soluble cap, a similar rate of inhibition was observed for products of both the sCAT and 3b ORFs (50–70% with 0.1 mM and 80–90% with 0.2 mM cap analog; Figs. 4B and 4D), mirroring the results with mRNA 3-like transcripts of pORF3a-3b-4 (Figs. 4A and 4C).
4. No translation of the remaining five ORFs was observed from either uncapped or capped transcripts.

These results show that translation of ORF 3b positioned 1263 nt downstream from the 5′ terminus in the synthetic construct is initiated by some form of internal entry of ribosomes and not by scanning, is influenced by a cap, and is not the result of a fragmented template.

Deletion analysis failed to identify a postulated IRES-like element within the upstream gene 3a

Although no universally identifying primary or secondary structural features of IRES elements are known, certain secondary structural features do appear necessary for IRES function (reviewed in Jackson, 1996). Within TGEV gene 3a, secondary structures can be predicted (Figs. 6A and 6B) that share features with the putative IRES element in IBV mRNA 3 (Liu and Inglis, 1992; Le *et al.,* 1995), leading us to postulate that gene 3a might contain an IRES. The predicted structures are five stem-loops (I–V), four of which can be drawn as components of pseudoknots. The free energies of these are calculated to be, respectively, −6.8, +6.0, −3.8, −0.8, and +5.6 kCal/mole by the algorithm of Tinoco *et al.* (1973), which

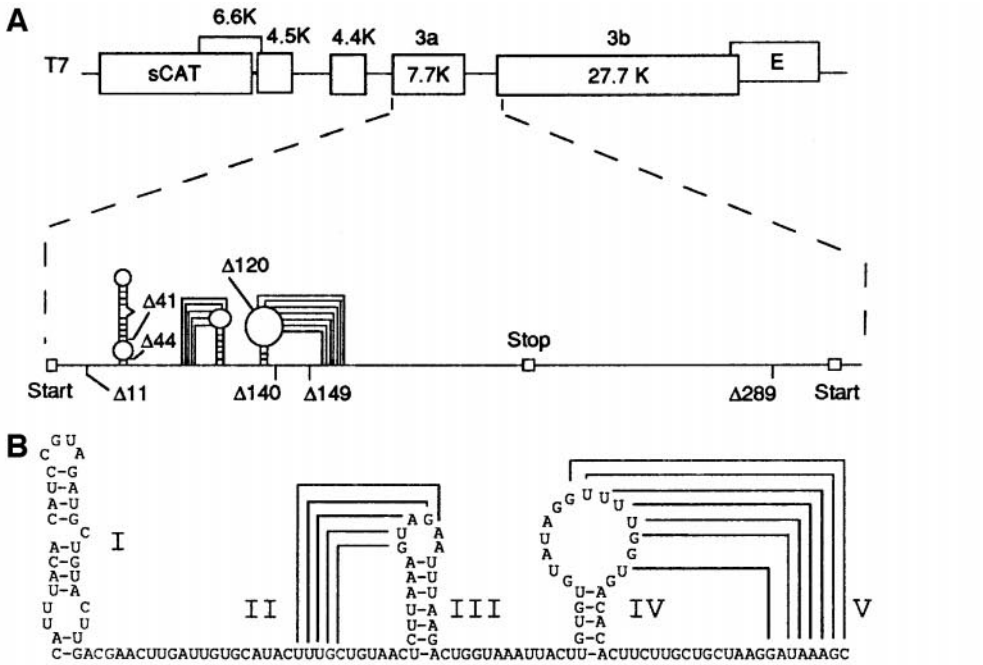
A
6.6K
4.5K
4.4K
3a
3b
T7
sCAT
7.7K
27.7 K
E
Δ120
Δ41
Δ44
Stop
Start
Δ11
Δ140
Δ149
Δ289
Start
B
I
II
III
IV
V
C-GACGAACUUGAUUGUGCAUACUUUGCUGUAACU-ACUGGUAAAUUACUU-ACUUCUUGCUGCUAAGGAUAAAGC

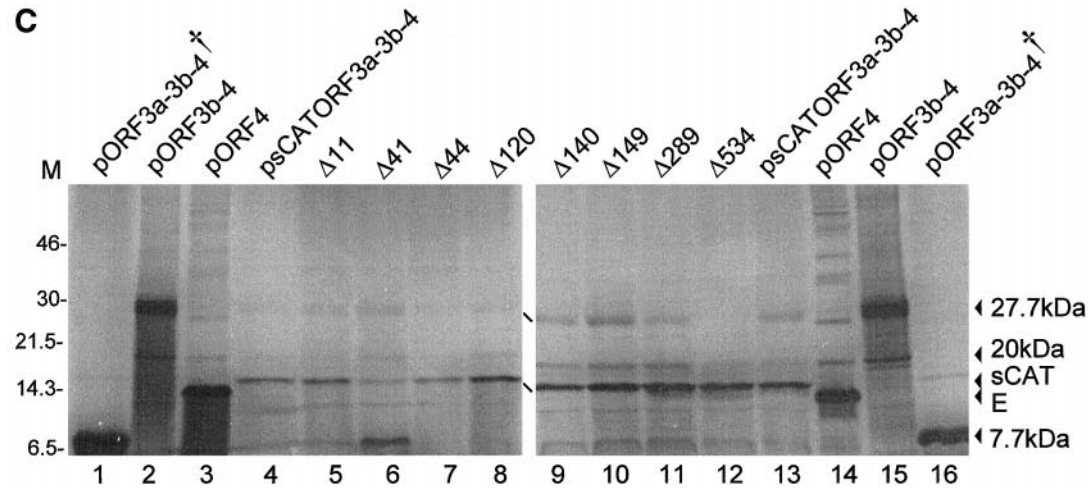
C
pORF3a-3b-4 †
pORF3b-4
pORF4
psCATORF3a-3b-4
Δ11
Δ41
Δ44
Δ120
Δ140
Δ149
Δ289
Δ534
psCATORF3a-3b-4
pORF4
pORF3b-4
pORF3a-3b-4 †
M
46-
30-
21.5-
14.3-
6.5-
27.7kDa
20kDa
sCAT
E
7.7kDa
1 2 3 4 5 6 7 8 9 10 11 12 13 14 15 16

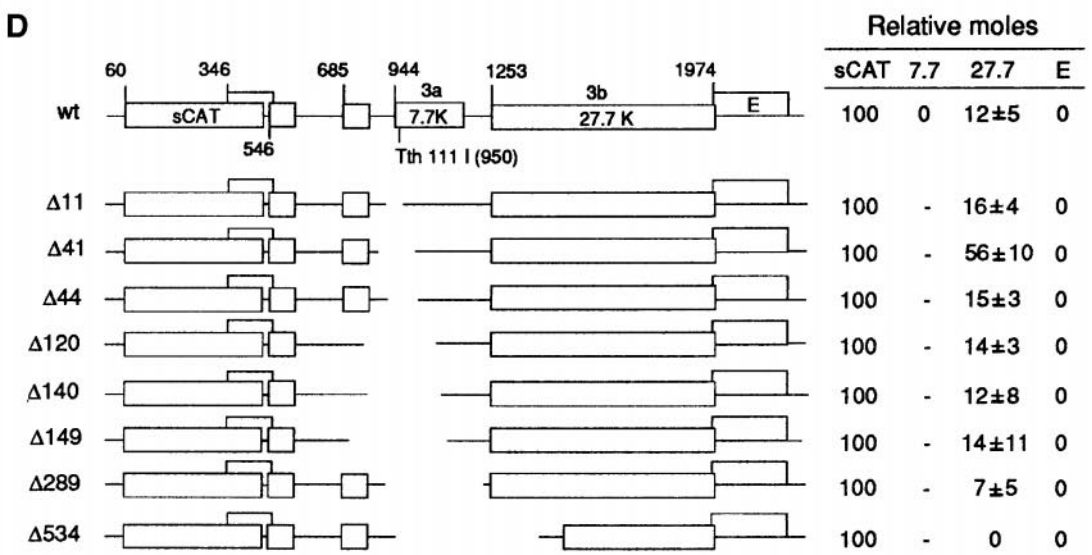
D
Relative moles
sCAT 7.7 27.7 E
60
346
685
944
1253
1974
wt
sCAT
3a
7.7K
3b
27.7 K
E
546
Tth 111 I (950)
Δ11 100 - 16±4 0
Δ41 100 - 56±10 0
Δ44 100 - 15±3 0
Δ120 100 - 14±3 0
Δ140 100 - 12±8 0
Δ149 100 - 14±11 0
Δ289 100 - 7±5 0
Δ534 100 - 0 0

are relatively unstable and suggest a low probability for their existence in viral RNA. Nevertheless, to test whether gene 3a might function as an IRES for translation of ORF 3b, deletions within it were prepared and tested. These were (mostly) bidirectional for distances of 16, 86, 74, 192, 314, 337, 334, and 523 nt, and represented 3′-ward deletions of 11, 41, 44, 120, 140, 149, 289, and 534 nt from the first nucleotide in gene 3a, respectively, for which the mutants were named. Results shown in Fig. 6C and summarized in Fig. 6D indicate that the relative molar amounts of sCAT and the 27.7-kDa gene 3b products (~1:0.12) remained essentially unchanged between wild-type and Δ149. The only exception was for Δ41, for which the molar ratio was 1:0.56 along with an inexplicable enhancement of an uncharacterized band with an approximate molecular weight of 6 kDa. For Δ289, which leaves only 17 nt upstream of the ORF 3b start codon, the relative amounts were surprisingly 1:0.07 and not 1:0, as expected. For Δ534, there was abundant synthesis of the sCAT protein but no synthesis of the 27.7-kDa protein; however, there was synthesis of the 20-kDa gene 3b product (O'Connor and Brian, 1999) (Fig. 6D). These results are not consistent with a mechanism of ribosomal entry within gene 3a but rather with one in which ribosomes enter within 50 nt from the start codon of gene 3b. Because the 20-kDa gene 3b product is found with mutant Δ534, the intriguing possibility exists that ribosomes are entering at or downstream of the gene 3b start site and are scanning in the upstream direction to reach the start codon.

DISCUSSION

Based on precedents in eukaryotes (reviewed in Mathews, 1996), four mechanistic possibilities should be considered as explanations for how ribosomes approach the downstream ORF 3b on TGEV mRNA 3 for translation: Ribosomes could (1) translate the upstream ORF and then reinitiate synthesis on the downstream ORF, (2) scan through the upstream ORF(s) without the act of translation in a manner known as leaky scanning, (3) bypass the upstream ORF(s) by using an internal ribosomal entry site similar to that used by picornaviruses and flaviviruses on genomic RNA, or (4) bypass the upstream ORF(s) after first binding to the mRNA in a cap-dependent manner and then undergo shunting to a downstream site on the mRNA. Among these, shunting is the most recently recognized and is exemplified by translation on pregenomic RNA of the cauliflower mosaic virus (Futterer *et al.,* 1993) and rice tungro bacilliform virus (Futterer *et al.,* 1996), both pararetroviruses, on adenovirus mRNA (Yueh and Schneider, 1996), and on Sendai paramyxovirus mRNA (Curran and Kolakovsky, 1988, 1989; Latorre *et al.,* 1998).

We conclude that ORF 3b is translated from mRNA 3, and that the likelihood is high that an internal entry of ribosomes is used, possibly one with shuntlike features, and perhaps in conjunction with leaky ribosomal scanning through ORF 3a. The relative contribution of each mechanism on mRNA 3 could not be established by the experiments performed here. However, an internal entry of ribosomes was demonstrated by the use of constructs, in which four extensive ORFs within an 884-nt sequence were placed upstream of ORF 3a and synthesis from ORF 3b was shown to remain approximately one-eighth to one-fifth of that from the 5′-terminal ORF. The internal entry showed some properties of shunting in that (1) no IRES element of the type directing internal entry in picornaviruses and togaviruses could be demonstrated within sequence upstream of gene 3b and (2) translation of ORF 3b in capped transcripts from the synthetic multicistronic psCATORF3a-3b-4 showed some inhibition by a competing soluble cap in the translation mix. That is, internal entry in the multicistronic transcript may follow a cap-dependent step as described for shunting in the adenoviruses, pararetroviruses, and paramyxoviruses.

In general, the mechanistic features of ribosomal shunting, so far described for only viral mRNAs (Jackson, 1996; Mathews, 1996), remain to be clarified. In the case of adenovirus and pararetrovirus mRNAs, an upstream donor structure appears necessary for the shunting step. In pararetrovirus, this appears to be a stable hairpin preceded by a short open reading frame (Hemmings-Mieszczak and Hohn, 1999). In the case of TGEV ORF 3b shunting reported here, a requirement for an upstream structure seems unlikely, since shunting took place in the presence of foreign sequence (psCATORF3a-3b-4) as well as (relatively) native sequence (pORF3a-3b-4) at the 5′ terminus. In this respect, the TGEV ORF 3b shunting pathway bears similarity to that in paramyxovirus mRNA, for which no apparent requirement for a donor structure was found (Latorre *et al.,* 1998). Likewise, it is not clear what determines the landing site in a ribosomal shunt. Certainly in the experiments reported here it is not apparent how ribosomes might have been directed to land so close to the 3b initiation codon in TGEV mRNA 3. It is

FIG. 6. Deletion analysis of the postulated IRES-like element within ORF 3a. (A and B) Postulated secondary structural elements within ORF 3a and map sites of the deletions used in expression analysis of ORF 3b. (C) Electrophoresis of translation products from the deletion mutants. † indicates plasmid DNA was linearized at the *Sca*I site within ORF 3b before transcription. (D) Summary of translation results from the deletion mutants of psCATORF3a-3b-4 along with a schematic diagram of the deletion mutants. No product of ORF 3a was expected (as indicated by −) because ORF 3a no longer existed after deletion mutagenesis.

clearly not the postulated secondary structures within gene 3a, because internal entry took place after these had been removed or disrupted (Δ149, Figs. 6C and 6D). One possibility is that ribosomes are directed to land at or near the start site of gene 3b by specific sequences or by higher-order structures situated very near the landing site. Precedents for this are found in Sendai virus, wherein sequences both upstream and downstream of the Y1 ORF are required for shunt landing (Latorre *et al.,* 1998), and in Hepatitis C virus, wherein sequences extending 28 nt into the ORF are required for IRES-directed landing (Reynolds *et al.,* 1995). Curiously, such a landing site might require that ribosomes backscan to find the gene 3b start codon, a process postulated to explain the translation of certain SV40 and influenza virus transcripts (Peabody *et al.,* 1986; Williams and Lamb, 1989).

Our findings were particularly intriguing because some evidence had suggested the existence of IRES-directed, cap-independent translation for the third ORF in tricistronic IBV mRNA 3 (Liu and Inglis, 1992; Le *et al.,* 1995) and for the second ORF in the bicistronic MHV mRNA 5 (Thiel and Siddell, 1994). The influence of the cap, however, was not examined in the MHV studies, and the possibility remains that a form of shunting might also be exhibited during the translation of these mRNAs.

The consequences of an internal ribosomal entry onto gene 3b for virus replication are not immediately apparent, but one might be that it enables a constitutive synthesis of 3b protein because, in principle, any of the viral mRNAs containing gene 3b (mRNAs 1, 2, and 3) could serve as templates.

MATERIALS AND METHODS

Cells and virus. The Purdue-116 and Miller strains of TGEV were obtained from E. Bohl, Ohio State University. Purdue-116 virus was plaque-purified from infectious genomic RNA, grown on swine testicle (ST) cells in medium containing 10% fetal calf serum (Atlanta Biologicals), and used within eight passages of plaque purification (Brian *et al.,* 1980; Kapke and Brian, 1986). Miller virus was similarly grown but was plaque-purified twice from infectious virus on ST cells and used within 10 passages of plaque purification.

Northern analysis of TGEV mRNAs. Northern analyses were performed as described (Sethna *et al.,* 1989) and quantitation was done with the AMBIS Photoanalytic Imaging System (AMBIS, San Diego, CA). Cells were infected with TGEV at a multiplicity of infection (m.o.i.) of 10 and total RNA was extracted at 6 and 9 h postinfection (hpi). Blots were probed with radiolabeled synthetic oligodeoxynucleotide specific for the leader (oligonucleotide L3+, 5′CGGGATCCTCGGGTTTAGTTCGAGTTGGTGTCCGAAGACAAAATCTAGCACAAGGCTAGTTAAAGTAAAAGAAGAGATAT3′), gene 3a (oligonucleotide 7.7, 5′GTTCGTCAAGTACAGCATCTACGG3′), or gene 3b (oligonucleotide 4, 5′CTTCTCATAAACGGTGCAGCTCTGCC3′). Probes were radiolabeled to a specific activity of 1.5 to 3.5 $\times$ 10^6 cpm/pmol by the forward reaction.

Construction of plasmids. TGEV Purdue sequences used in this study have been published (Kapke, *et al.,* 1988a; Sethna *et al.,* 1991). The construction of pORF3b-4 (Fig. 1C), formerly called pORF2, has been described (O'Connor and Brian, 1999). pORF3b-4 carries genes 3b and 4 and 308 nt of gene 5 in vector pGEM-4Z (Promega Biotech) (a sequence obtained from cDNA clone pFT44 [Fig. 1A]). pORF4 (Fig. 1C) was made from pORF3b-4 by first removing the 291-nt M-containing *Sph*I fragment, religating, and then removing the 716-nt *Hin*dIII-*Bbs*I fragment and religating after blunt-ending with mung bean nuclease. pORF3a-3b-4 (Fig. 1C), which carries genes 3a, 3b, and 4 downstream of the T7 RNA polymerase promoter in pGEM-3Z (Promega Biotech), was made in three steps. First, pSP6ORF3a, from which gene 3a and 591 nt of gene 3b can be transcribed with RNA polymerase SP6, was created by ligating the 1111 bp *Nsi*I-*Pst*I fragment from clone pFT39 (a clone containing nucleotides 3968 to 5449 from the genome 3′ end [Fig. 1A; Tung *et al.,* 1992], prepared as described in Kapke *et al.,* 1988a,b) into the *Pst*I site of pGEM-3Z. Second, pSP6ORF3a-3b-4 was created by ligating the 925-bp *Bsr*GI-*Eco*RI fragment from pORF3b-4 into the 4048-nt vector-containing *Eco*RI-*Bsr*GI-linearized fragment of pSP6ORF3a. Third, the entire 1340-nt *Sph*I-*Hin*fI insert from pSP6ORF3a-3b-4, after blunt-ending with T4 DNA polymerase, was ligated in the reverse orientation into similarly blunt-ended *Eco*RI-*Sac*I-linearized pGEM-3Z.

To place the viral leader upstream of ORF 3a, pLORF3a-3b-4 (Fig. 1C) was constructed by a previously published procedure (Sethna *et al.,* 1991; Hofmann *et al.,* 1993). Briefly, cDNA was made from the 5′ end of mRNA 3 with a primer specific to gene 3b (oligo 4(+) [5′CTTCTCATAAACGGTGCAGCTCTGCC3′]), and amplified by PCR using oligo 4(+) and oligo leaderGAC(−) (5′GCGGGCCCGGGACTTTTAAAGTAAAG3, which binds to the minus-strand of the leader), to create a leader-containing fragment. The product was digested with *Sma*I and *Bsr*GI, and the large fragment was ligated in a three-way ligation reaction with the 590-nt *Bsr*GI-*Sph*I fragment of pORF3a-3b, and with pGEM-4Z that had been linearized with *Hin*dIII, blunt-ended with T4 DNA polymerase, and digested with *Sph*I.

To create a strong Kozak context for the 3a start codon, thus creating pORF3a(K)-3b-4, an overlap PCR mutagenesis procedure (Horton *et al.,* 1990) was used. For this, complementary mutagenesis primers 7.7Kozak(+) (5′CAATGTCAATGGTGGCCCTGTAATGAC3′) and 7.7Kozak(−) (5′GTCATTACAGGGCCACCATGGACATTG3′), and primers oligo 5(+) (5′TGCCACCATACAATGTGACA3′, which binds to bases 465–484 within ORF 3b) and pGEM3Zf(−)*Nde*I(−) (5′GAGAGTGCACCATATGCGGTGT3′, which binds to bases 2498–2519 within pGEM-3Z), were used together in

the overlap procedure to amplify a 1066-nt product from pORF3a-3b-4 DNA. After digestion with restriction enzymes *Nar*I and *Bsr*GI, the 932-nt product was cloned into *Nar*I-*Bsr*GI-linearized pORF3a-3b-4.

To create pCATORF3a-3b-4 (Fig. 1C), the ORF3a-3b-4-containing 1534-nt *Sph*I fragment from pORF3a-3b-4 was placed into the *Sph*I site of pCAT (Fig. 1C), which was made by cloning the *Bam*HI fragment from pCM4 (Pharmacia) into the *Bam*HI site of pGEM-3Z. For better size resolution of the large proteins, the CAT gene in pCATORF3a-3b-4 was truncated by 91 nt on its 3′ end by digestions with *Nco*I and nuclease Bal 31, thus forming psCATORF3a-3b-4 (Fig. 1C). This, along with a frameshift, resulted in a total shortening of the CAT protein (now called sCAT) by 46 aa.

The junctions of all constructs were confirmed by sequencing plasmid DNA.

Preparation of nested deletions within gene 3a, the postulated internal ribosomal entry region. To obtain deletions within gene 3a, psCATORF3a-3b-4 DNA was linearized at base 7 of ORF 3a with Tth111 I, treated with Bal 31 and mung bean nucleases, purified by electrophoresis, and religated. Transformants were screened for deletions by PCR and the sequenced constructs were named for the number of bases deleted downstream of the gene 3a start site (the total number of deleted bases is also noted).

In vitro translation and analysis of products. In vitro transcription with T7 RNA polymerase was carried out on linearized plasmid DNAs as recommended (Promega Biotech). pORF3b-4 was linearized with *Eco*RI, pORF3a-3b-4 with *Sca*I or *Bam*HI, as indicated, and psCATORF3a-3b-4 with *Ase*I. The 1274-nt DNA fragment from *Sca*I-linearized pORF3a-3b-4 was purified by affinity chromatography (Geneclean; Bio 101) to ensure transcription of only ORF 3a. For preparation of capped RNA transcripts, 0.5 mM m7G(5′)ppp(5′)G and 0.25 mM GTP replaced 2.5 mM GTP in the transcription mix (Promega Biotech). Each preparation of RNA was purified by Biospin column chromatography (Bio-Rad), quantitated by spectrophotometry, and monitored for degradation by agarose gel electrophoresis. *In vitro* translation was carried out in methionine-depleted wheat germ extracts or rabbit reticulocyte lysates as recommended by the manufacturers (Promega Biotech and Ambion, Inc.). In some preparations, translation products were treated with RNase A before electrophoresis as recommended by Ambion, Inc., to remove a 27-kDa endogenous band caused by the binding of charged tRNA to proteins. Fifty-microliter reaction volumes contained 50 μCi ^{35}S-methionine (1000 Ci/mmol; ICN) and 1.0 μg of RNA transcript. To test for inhibition of translation by exogenous methylated cap analog, m7G(5′)ppp(5′)G (New England Biolabs) was added to the translation mix to final concentrations of 0.1, 0.2, 0.4, and 0.8 mM. Radioactivity in the separated products was quantitated by scanning dried gels with the AMBIS Photoanalytic Imaging System (San Diego, CA) or by scanning autoradiograms of the gels with the Bio-Rad Imaging Spectrophotometer (Bio-Rad). Each experiment depicted was done minimally on three separate preparations of transcript RNA. Standard deviation measurements were made from the results of three separate experiments.

ACKNOWLEDGMENTS

We thank Seulah Ku and Gwyn Williams for the construction of pCAT. This work was supported by Public Health Service Grant AI 14367 from the National Institutes of Health and Grant 92-37204-8046 from the U.S. Department of Agriculture, and in part with funds from the University of Tennessee College of Veterinary Medicine Center of Excellence Program for Livestock Diseases and Human Health.

REFERENCES

Boursnell, M. E. G., Binns, M. M., and Brown, T. D. K. (1985). Sequencing of coronavirus IBV genomic RNA: Three open reading frames in the 5′ "unique" region of mRNA D. *J. Gen. Virol.* **66,** 2253–2258.

Brian, D. A., Dennis, D. E., and Guy, J. S. (1980). Genome of porcine transmissible gastroenteritis virus. *J. Virol.* **34,** 410–415.

Brierly, I., Boursnell, M. E. G., Binns, M. M., Bilimoria, B., Blok, V. C., Brown, T. D. K., and Inglis, S. C. (1987). An efficient ribosomal frame-shifting signal in the polymerase-encoding region of the coronavirus IBV. *EMBO J.* **6,** 3779–3785.

Britton, P., Lopez Otin, C., Martin Alonso, J. M., and Parra, F. (1989). Sequence of the coding regions from the 3.0 kb and 3.9 kb mRNA subgenomic species from a virulent isolate of transmissible gastroenteritis virus. *Arch. Virol.* **105,** 165–178.

Budzilowicz, C. J., and Weiss, S. R. (1987). In vitro synthesis of two polypeptides from a nonstructural gene of coronavirus mouse hepatitis virus strain A59. *Virology* **157,** 509–515.

Chen, C.-M., Cavanagh, D., and Britton, P. (1995). Cloning and sequencing of an 8.4 kb region from the 3′ end of a Taiwanese virulent field isolated of the coronavirus transmissible gastroenteritis virus (TGEV). *Virus Res.* **38,** 83–89.

Curran, J., and Kolakovsky, D. (1988). Scanning independent ribosomal initiation of the Sendai virus X protein. *EMBO J.* **7,** 2869–2874.

Curran, J., and Kolakovsky, D. (1989). Scanning independent ribosomal initiation of the Sendai virus Y proteins in vitro and in vivo. *EMBO J.* **8,** 521–526.

Eleouet, J. F., Rasschaert, D., Lambert, P., Levy, L., Vende, P., and Laude, H. (1995). Complete sequence (20 kilobases) of the polyprotein-encoding gene 1 of transmissible gastroenteritis virus. *Virology* **206,** 817–822.

Enjuanes, L., and Van der Zeijst, B. A. M. (1995). Molecular basis of transmissible gastroenteritis coronavirus (TGEV) epidemiology. *In* "The Coronaviridae" (S. G. Siddell, Ed.), pp. 337–376. Plenum, New York.

Fischer, F., Peng, D., Hingley, S. T., Weiss, S. R., and Masters, P. S. (1997). The internal open reading frame within the nucleocapsid gene of mouse hepatitis virus encodes a structural protein that is not essential for viral replication. *J. Virol.* **71,** 996–1003.

Futterer, J., Kiss-Laszio, Z., and Hohn, T. (1993). Nonlinear ribosome migration on cauliflower mosaic virus 35S RNA. *Cell* **73,** 789–802.

Futterer, J., Potrykus, I., Bao, Y., Li, L., Burns, T. M., Hull, R., and Hohn, T. (1996). Position-dependent ATT initiation during plant pararetrovirus rice tungro bacilliform virus translation. *J. Virol.* **70,** 2999–3010.

Hemmings-Mieszczak, M., and Hohn, T. (1999). A stable hairpin preceded by a short open reading frame promotes nonlinear ribosome migration on a synthetic mRNA leader. *RNA* **5,** 1149–1157.

Hofmann, M. A., Chang, R.-Y., and Brian, D. A. (1993). Leader-mRNA

junction sequences are unique for each subgenomic mRNA species in the bovine coronavirus and remain so throughout persistent infection. *Virology* **196,** 163–171.

Horton, R. M., Zeling, C., Steffan, N. H., and Bease, L. R. (1990). Gene splicing by overlap extension: Tailor-made genes using polymerase chain reaction. *BioTechniques* **8,** 528–535.

Iizuka, N., Najita, L., Franzusoff, A., and Sarnow, P. (1994). Cap-dependent and cap-independent translation by internal initiation of mRNAs in cell extracts prepared from *Saccharomyces cerevisiae*. *Mol. Cell. Biol.* **14,** 7322–7330.

Jackson, R. J. (1996). A comparative view of initiation site selection mechanisms. *In* "Translational Control" (J. W. B. Hershey, M. B. Mathews, and N. Sonenberg, Eds.), pp. 71–112. Cold Spring Harbor Laboratory Press, Cold Spring Harbor, New York.

Jackson, R. J., Hunt, S. C., Reynold, J. E., and Kaminski, A. (1995). Cap-dependent and cap independent translation: Operational distinctions and mechanistic interpretations. *In* "Current Topics in Microbiology and Immunology: Cap-independent Translation" (P. Sarnow, Ed.), pp. 1–29. Springer-Verlag, New York.

Kapke, P. A., and Brian, D. A. (1986). Sequence analysis of the porcine transmissible gastroenteritis coronavirus nucleocapsid protein gene. *Virology* **151,** 41–49.

Kapke, P. A., Tung, F. Y. T., and Brian, D. A. (1988a). Nucleotide sequence between the peplomer and matrix protein genes of the porcine transmissible gastroenteritis coronavirus identifies three large open reading frames. *Virus Genes* **2,** 293–294.

Kapke, P. A., Tung, F. Y. T., Hogue, B. G., Brian, D. A., Woods, R. D., and Wesley, R. (1988b). The amino-terminal signal peptide on the porcine transmissible gastroenteritis coronavirus matrix protein is not an absolute requirement for membrane translocation and glycosylation. *Virology* **165,** 367–376.

Kozak, M. (1989). The scanning model for translation: An update. *J. Cell Biol.* **108,** 229–241.

Kozak, M. (1991a). An analysis of vertebrate mRNA sequences: Intimations of translational control. *J. Cell Biol.* **115,** 887–903.

Kozak, M. (1991b). Structural features in eukaryotic mRNAs that modulate the initiation of translation. *J. Biol. Chem.* **266,** 19867–19870.

Lai, M. M. C., and Cavanagh, D. (1997). The molecular biology of coronaviruses. *Adv. Virus Res.* **48,** 1–100.

Latorre, P., Kolakofsky, D., and Curran, J. (1998). Sendai virus Y proteins are initiated by a ribosomal shunt. *Mol. Cell. Biol.* **18,** 5021–5031.

Le, S.-Y., Sonenberg, N., and Maizel, J. V. (1995). Distinct structural elements and internal entry of ribosomes in mRNA 3 encode by infectious bronchitis virus. *Virology* **198,** 405–411.

Leibowitz, J. L., Perlman, S., Weinstock, G., DeVries, J. R., Budzilowitz, C., Weisseman, J. M., and Weiss, S. R. (1988). Detection of a murine coronavirus nonstructural protein encoded in a downstream open reading frame. *Virology* **164,** 156–164.

Liu, D. X., Cavanagh, D., Green, P., and Inglis, S. C. (1991). A polycistronic mRNA specified by the coronavirus infectious bronchitis virus. *Virology* **184,** 531–544.

Liu, D. X., and Inglis, S. C. (1992). Internal entry of ribosomes on a tricistronic mRNA encoded by infectious bronchitis virus. *J. Virol.* **66,** 6143–6154.

Luytjes, W. (1995). Coronavirus gene expression: Genome organization and protein synthesis. *In* "The Coronaviridae" (S. G. Siddell, Ed.), pp. 33–54. Plenum, New York.

Mathews, M. B. (1996). Interactions between viruses and the cellular machinery for protein synthesis. *In* "Translational Control" (J. W. B. Hershey, M. B. Mathews, and N. Sonenberg, Eds.), pp. 505–548. Cold Spring Harbor Laboratory Press, Cold Spring Harbor, New York.

O'Connor, J. B., and Brian, D. A. (1999). The major product of porcine transmissible gastroenteritis coronavirus gene 3b is an integral membrane glycoprotein of 31 kDa. *Virology* **256,** 152–161.

Peabody, D. S., Subramani, S., and Berg, P. (1986). Effect of upstream reading frames on translation efficiency in simian virus 40 recombinants. *Mol. Cell. Biol.* **6,** 2704–2711.

Rasschaert, D., Gelfi, J., and Laude, H. (1987). Enteric coronavirus TGEV: Partial sequence of the genomic RNA, its organization and expression. *Biochimie (Paris)* **69,** 591–600.

Reynolds, J. E., Kaminski, A., Kettinen, H. J., Grace, K., Clarke, B. E., Carroll, A. R., Rowlands, D. J., and Jackson, R. J. (1995). Unique features of internal initiation of hepatitis C virus RNA translation. *EMBO J.* **14,** 6010–6020.

Senanayake, S. D., and Brian, D. A. (1997). Bovine coronavirus I protein synthesis follows ribosomal scanning on the bicistronic N mRNA. *Virus Res.* **48,** 101–105.

Senanayake, S. D., Hofmann, M. A., Maki, J. L., and Brian, D. A. (1992). The nucleocapsid gene of bovine coronavirus is bicistronic. *J. Virol.* **66,** 5277–5283.

Sethna, P. B., Hofmann, M. A., and Brian, D. A. (1991). Minus-strand copies of replicating coronavirus mRNAs contain antileaders. *J. Virol.* **65,**320–325.

Sethna, P. B., Hung, S.-L., and Brian, D. A. (1989). Coronavirus subgenomic minus-strand RNA and the potential for mRNA replicons. *Proc. Natl. Acad. Sci. USA* **86,** 5626–5630.

Skinner, M. A., Ebner, D., and Siddell, S. G. (1985). Coronavirus MHV-JHM mRNA 5 has a sequence arrangement which potentially allows translation of a second downstream open reading frame. *J. Gen. Virol.* **66,** 581–592.

Thiel, V., and Siddell, S. G. (1994). Internal ribosomal entry in the coding region of murine hepatitis virus mRNA 5. *J. Gen. Virol.* **75,** 3041–3046.

Tinoco, I., Borer, P. N., Dengler, B., Levine, M. D., Uhlenbeck, O. C., Crothers, D. M., and Gralla, J. (1973). Improved estimation of secondary structure in ribonucleic acids. *Nature* **246,** 40–41.

Tung, F. Y. T., Abraham, S., Sethna, M., Hung, S.-L., Sethna, P. B., Hogue, B. G., and Brian, D. A. (1992). The 9.1 kilodalton hydrophobic protein encoded at the 3′ end of the porcine transmissible gastroenteritis coronavirus genome is membrane associated. *Virology* **186,** 676–683.

Vaughn, E. M., Halbur, P. G., and Paul, P. S. (1995). Sequence comparison of porcine respiratory coronavirus isolates reveals heterogeneity in the S, 3, and 3–1 genes. *J. Virol.* **69,** 3176–3184.

Wesley, R. D., Cheung, A. K., Michael, D. D., and Woods, R. D. (1989). Nucleotide sequence of coronavirus TGEV genomic RNA: Evidence for 3 mRNA species between the peplomer and matrix protein genes. *Virus Res.* **13,** 87–100.

Wesley, R. D., Woods, R. D., and Cheung, A. K. (1990). Genetic basis for the pathogenesis of transmissible gastroenteritis virus. *J. Virol.* **64,** 4761–4766.

Wesley, R. D., Woods, R. D., and Cheung, A. K. (1991). Genetic analysis of porcine respiratory coronavirus, an attenuated variant of transmissible gastroenteritis virus. *J. Virol.* **65,** 3369–3373.

Williams, M. A., and Lamb, R. A. (1989). Effect of mutations and deletions in a bicistronic mRNA on the synthesis of influenza B virus NB and NA glycoproteins. *J. Virol.* **63,** 28–35.

Yueh, A., and Schneider, R. J. (1996). Selective translation initiation by ribosome jumping in adenovirus-infected and heat-shocked cells. *Genes Dev.* **10,** 1557–1567.